

RS-8232-2/62792

SANDIA REPORT

SAND85-0023 • Unlimited Release • UC-70

Printed August 1985

C.1



8232-2/062792



00000001 -

Marker Bed 139: A Study of Drillcore From A Systematic Array

David J. Borns

Prepared by
Sandia National Laboratories
Albuquerque, New Mexico 87185 and Livermore, California 94550
for the United States Department of Energy
under Contract DE-AC04-76DP00789



865852/867832

Issued by Sandia National Laboratories, operated for the United States Department of Energy by Sandia Corporation.

NOTICE: This report was prepared as an account of work sponsored by an agency of the United States Government. Neither the United States Government nor any agency thereof, nor any of their employees, nor any of their contractors, subcontractors, or their employees, makes any warranty, express or implied, or assumes any legal liability or responsibility for the accuracy, completeness, or usefulness of any information, apparatus, product, or process disclosed, or represents that its use would not infringe privately owned rights. Reference herein to any specific commercial product, process, or service by trade name, trademark, manufacturer, or otherwise, does not necessarily constitute or imply its endorsement, recommendation, or favoring by the United States Government, any agency thereof or any of their contractors or subcontractors. The views and opinions expressed herein do not necessarily state or reflect those of the United States Government, any agency thereof or any of their contractors or subcontractors.

Printed in the United States of America
Available from
National Technical Information Service
U.S. Department of Commerce
5285 Port Royal Road
Springfield, VA 22161

NTIS price codes
Printed copy: A03
Microfiche copy: A01

Marker Bed 139: A Study of Drillcore From A Systematic Array

David J. Borns
Earth Sciences Division
Sandia National Laboratories
Albuquerque, NM 87185

Abstract

In southeastern New Mexico, Marker Bed 139 (referred to in this report as MB139) is one of 45 numbered siliceous or sulfatic units within the Salado Formation of the northern Delaware Basin. MB139 is divided into five zones. Zones I and V are the upper and lower contact zones, respectively. Zone II is a syndepositionally deformed subunit of polyhalitic anhydrite. Zone III is mixed anhydrite and polyhalitic anhydrite, a distinctive pale-green and pink, with subhorizontal fractures. Zone IV consists of interlayered halite and anhydrite without the overprint of polyhalite.

This sequence was transitional between submarine and subaerial. The anhydritic units of MB139 formed in salt-pan or mudflat environments or both. Undulations observed along the upper contact of MB139 are interpreted to result from traction deposits or from reworking of the upper portion of the marker bed during the transition from anhydrite to halite deposition. Zones II and III exhibit soft-sediment deformation and later traces of dewatering; e.g., formation of stylolites. Such deformation is not observed in the halite above MB139 or in Zone V and the halite units below MB139.

A distinctive set of subhorizontal fractures occurs in MB139 in mid-Zone III and, to some extent, in Zone IV. These fractures are partially infilled with halite and polyhalite. Brine occurrences at the mined facility horizon at the Waste Isolation Pilot Plant may be related to these fractures. The fractures formed either in response to stress cycles that were functions of sedimentation and erosion, or in response to deformation in the underlying Castile Formation. The subhorizontal orientation, dominant in the sampling to date, is more consistent with the interplay between stress and sedimentation cycles.

Acknowledgments

C. L. Christensen and F. E. Hensley of Division 6332 helped immensely by setting up the drilling program at the WIPP site. The actual drilling was done by many Sandia and Technical Service Contractor personnel to whom I am grateful. F. E. Hensley was also of great help later in preparing samples for description and photography. M. Edwards of Tech Reqs drew the excellent graphics for the core description. J. C. Lorenz of Division 6253 and C. L. Stein of Division 6331 provided thoughtful reviews that helped clarify this report.

Contents

Introduction	7
Stratigraphy	7
Statement of the Problem	7
Fluids Associated With MB139	9
Methods of Study	9
Description	9
Core of Five-Hole Array in Room 4	9
Bounding Halite Units	14
Discussion of the Origin of Undulations on the Upper Surface of MB139	15
Conclusions	21
References	22
APPENDIX—Mesoscopic Description of the MB139 Core From the Five-Hole Array in Room 4	23

Figures

1	Cross section (after Jarolimek et al, 1983) from DOE-1 to the WIPP site, southeast to northwest	8
2	Plan view, north end of Room 4, with distribution of holes in the five-hole array	9
3	The five zones of MB139, shown in an idealized core section	10
4	Descriptive logs for core from the five-hole array	11
5	Multiple partial or complete bands, B1 to B3, of swallowtail growth in Hole 5, 5 ft, in which the adjacent bands are not contorted harmonically	16
6	Accumulation of hopper crystals within the upper contract Zone I of MB139, with intergranular polyhalite and secondary veining	17
7	Gypsum growth structures evident in the MB139 section	17
8	Inclined laminations in Zones I through III	18
9	Crenulated stylolitic laminae and pullaparts of anhydrite laminae in Zone IV	19
10	Overburden from the Permian to the present above the Rustler-Dewey Lake contact, which is the highest major marker without effects of post-Permian erosion	19

Marker Bed 139: A Study of Drillcore From A Systematic Array

Introduction

Stratigraphy

Within the northern Delaware Basin of southeastern New Mexico, the Salado Formation of Ochoan age occurs between the overlying Rustler Formation and the underlying Castile Formation (Figure 1). The Salado is primarily halite and consists of three sub-units: the upper, middle, and lower Salado. The stratigraphic nomenclature and usage in this report originated in the local potash industry (Jones et al, 1960). The boundaries of these subunits are the Rustler-Salado contact and Marker Bed 124 for the upper Salado, Marker Beds 124 and 136 for the middle Salado, and Marker Bed 136 and the Salado-Castile contact for the lower Salado. The lower Salado also includes the Cowden Anhydrite and the Infra-Cowden Halite. Within the Salado, Marker Bed 139 (referred to in this report as MB139) is one of 45 siliceous or sulfatic units numbered 100 to 145, with Marker Bed 145 occupying the lowest position stratigraphically. Such marker beds are traceable in the subsurface for several kilometers, although they are not recognizable in every hole.

The Salado is part of the paleo-environmental transition from marine and reefoid limestones to redbeds in the Ochoan series of the northern Delaware Basin (Jones and Madsen, 1968). In this transitional sequence, the Salado represents cycles of flooding and desiccation. With such cycles, a repetition of lithologic sequence is observed (Lowenstein, 1982). Typically, the Salado is comprised of rhythmically interlayered halite and argillaceous halite. Thinner units, comprised of anhydrite or other minerals such as polyhalite and clay, are also observed. Distinctive associations of rock types such as a claystone occur at the base of nearly every anhydrite unit. Jones and Madsen (1968) interpreted the claystone as the bottom, or start, of a sedimentary cycle. In such cycles, the ideal mineral sequence upwards is magnesite, anhydrite, polyhalite, glauberite, halite, and argillaceous halite. The upper boundary of this cycle is a fairly even surface, the result of corrosion or dissolution (Lowenstein, 1982).

Statement of the Problem

During early development of the underground Waste Isolation Pilot Plant (WIPP) facility, Jarolimek et al (1983) reported that MB139 exhibited an undulatory upper surface in several shafts and vertical boreholes. These undulations were reported to have vertical amplitudes of ~20 in. and wavelengths of 2 to 6 ft.*

The Environmental Evaluation Group (EEG) of the State of New Mexico expressed concern that, since MB139 was a short distance below the facility level (<3 m), these undulations may be evidence of some deformational event that affected the repository level at a stage later than deposition or diagenesis. Jarolimek et al (1983), however, argued that the undulations on the upper surface of MB139 were formed during deposition. They suggested the following as evidence for their conclusion:

- Laminations in halite-rich bands immediately above MB139 are horizontal and undeformed.
- Undulations on the lower contact of MB139 are minor relative to those on the upper surface of MB139.

Powers (in Jarolimek et al, 1983) concluded that the undulations were related to gypsum growth structures that formed shortly after or during deposition. These growth structures are observed as distinctive swallowtail clusters in which the original gypsum is now pseudomorphed by halite.

As an expansion of the work described above, the objective of this report was to assess our understanding of MB139 and to record a systematic drilling program to study MB139. The remaining basic questions addressed in this report follow:

*In this text, we use both English and metric units. The Jarolimek et al report uses English units, and I have reproduced their description. I use metric units for original observations within this report where possible. But, as with any area that incorporates oil-field and engineering projects, much of the original data appears in English units.

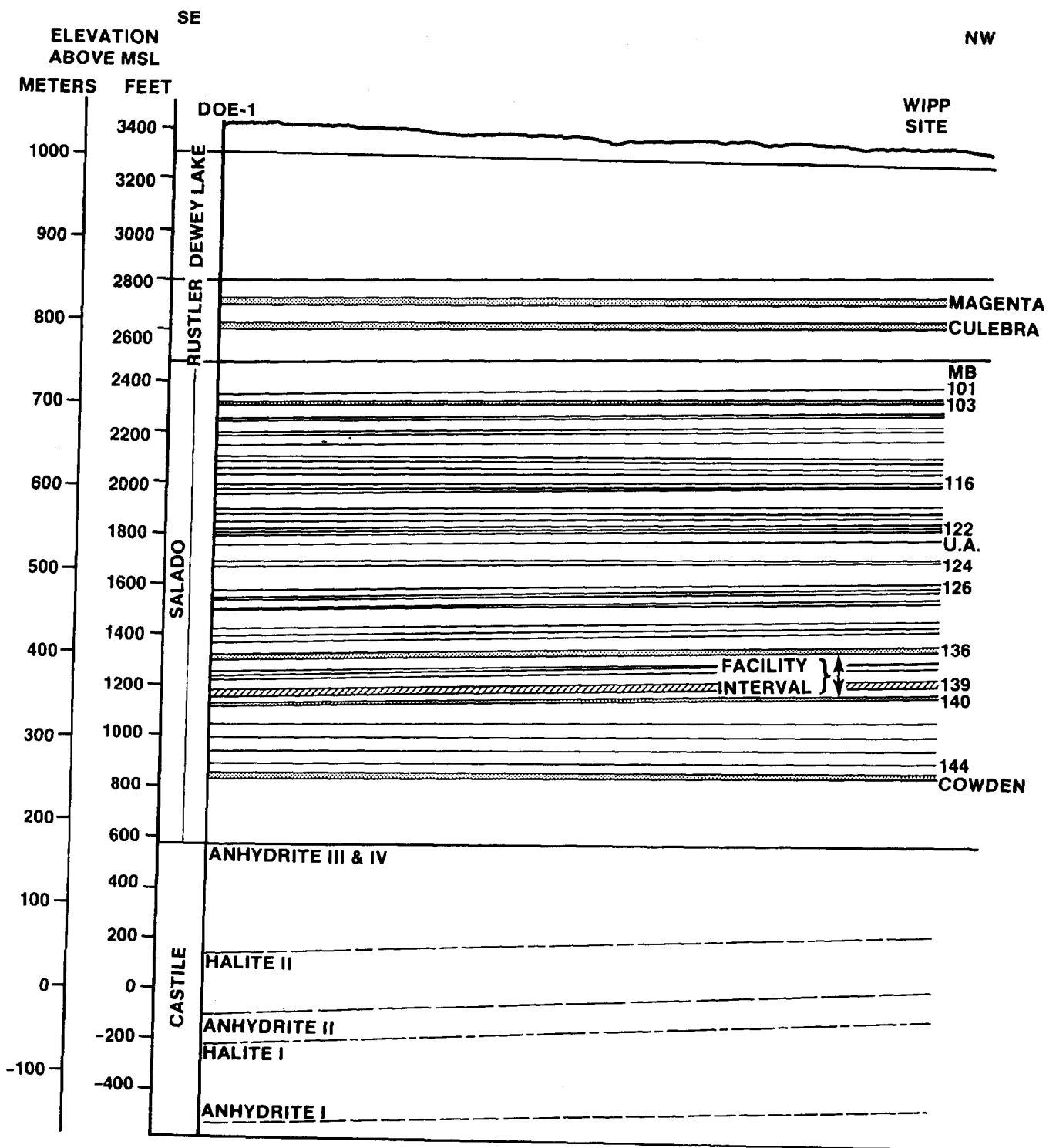


Figure 1. Cross section (after Jarolimek et al, 1983) from DOE-1 to the WIPP site, southeast to northwest. (The distribution of marker beds is illustrated in Salado.)

- What is the origin of the undulations on the top surface of MB139—regional deformation or deposition? What are the strengths and weaknesses of the arguments advanced by Jarolimek et al?
- What evidence remains in MB139 of the depositional and deformational history of the middle Salado?
- Are the mechanical responses of anhydritic units such as MB139 different responses of the halitic units that bound units such as MB139; e.g., brittle vs ductile behavior? Are meso- and microscopic textures observable in units such as MB139 that indicate such differing mechanical behavior for the units in question?
- Can MB139 and other similar units serve as local reservoirs for brines in the middle Salado?

Fluids Associated With MB139

Another point of interest about MB139 and similar units is the discovery of brines in drillholes that intersect MB139. These brines are also associated with predominantly nitrogen gas encounters at the facility interval, which is the mined underground workings of WIPP (Figure 1). In fact, the brine was discovered during a gas-drilling program within the underground facility (Popielak, 1983).

The initial hole that produced fluids was monitored and found to repressurize to >100 psi. This relationship between MB139 and the fluids or gases is being investigated through the auspices of the Technical Support Contractor (TSC). The TSC program incorporates recommendations of this author and others.

Methods of Study

Samples for this report came primarily from a five-hole array drilled in Room 4 (Figure 2). The core diameter in this array was 4 in. MB139 was generally 2 to 3 ft below the floor of Room 4. Other observations were made in 30- and 36-in. holes drilled through the marker bed in Room 4. The core from 16-in. drillholes in Room 4 was also available at the site for study. The larger diameter holes lie 15 to 20 m south of the five-hole array in Room 4. The core was described, and significant features were photographed. At this stage, samples were selected for thin sections, and 0.25-in.-thick slabs were cut from these samples. The samples were coated on one side with Buehler cold-mount epoxy to buttress the section for final slabbing. The slabs were trimmed to 2 or 3 in. and thinned to 0.125 in. The work herein is derived from mesoscopic

description of the core and finished slabs. No microscopic descriptions of MB139 core are included in this report.

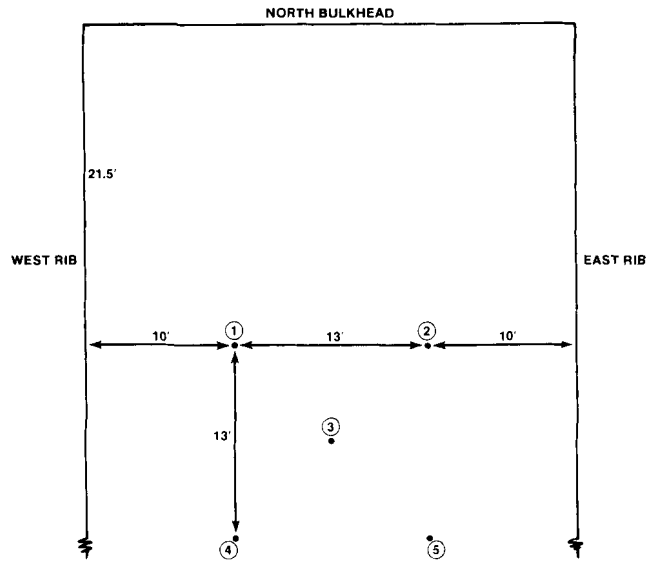


Figure 2. Plan view, north end of Room 4, with distribution of holes in the five-hole array

Description

Core of Five-Hole Array in Room 4

The detailed observations of the core obtained in the five-hole array in Room 4 appear in the Appendix and graphically in Figures 3 and 4. Stratigraphically, MB139 is divisible into five zones. The boundaries of these zones are generally gradational except for some sharp color contrasts; e.g., red to grey. The undulation structures, which originally spurred interest in MB139, are confined to the upper Zone I (described below). Other undulatory structures occur in zones stratigraphically lower within the marker bed. These lower structures are not necessarily harmonic; e.g., axial planes are not coplanar with the undulations in the upper zone. As an overview, the basic zones of MB139 are as follows:

<u>Zone</u>	<u>Zone Description</u>
I	Upper contact zone
II	Massive polyhalitic anhydrite
III	Mixed anhydrite and polyhalitic anhydrite
IV	Laminated anhydrite with halite
V	Lower contact zone

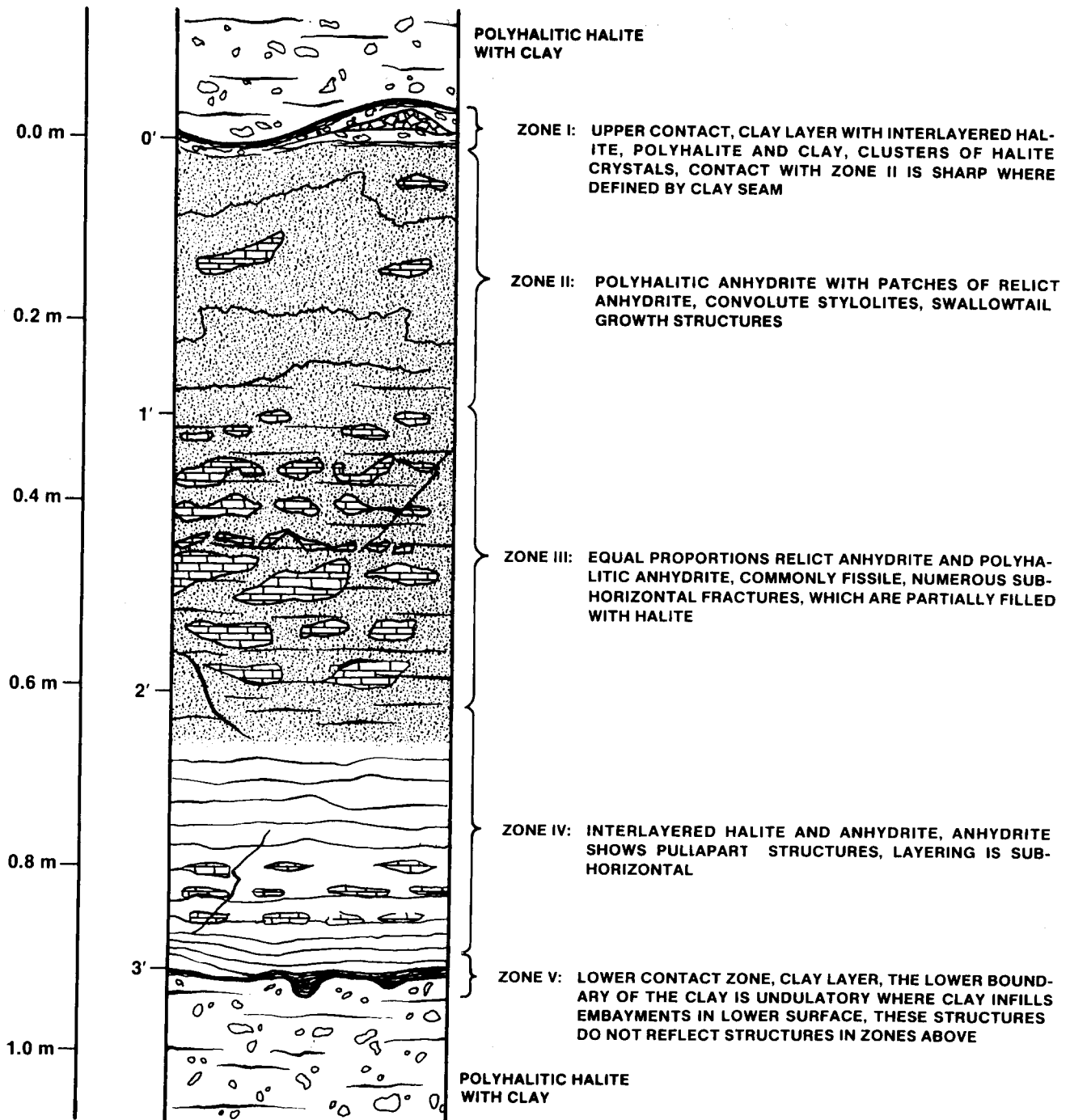


Figure 3. The five zones of MB139, shown in an idealized core section

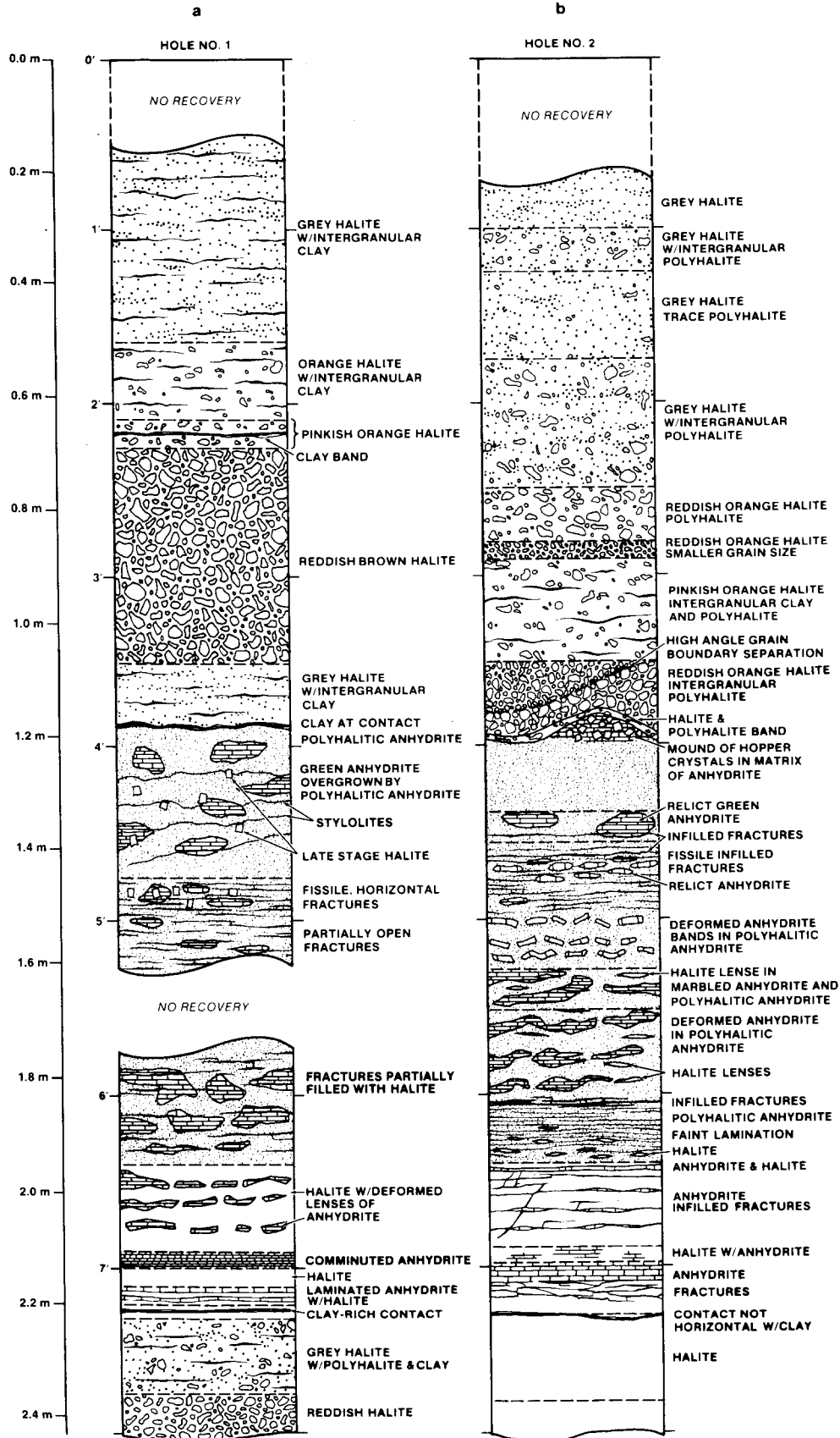


Figure 4. Descriptive logs for core from the five-hole array (detailed description appears in the Appendix)

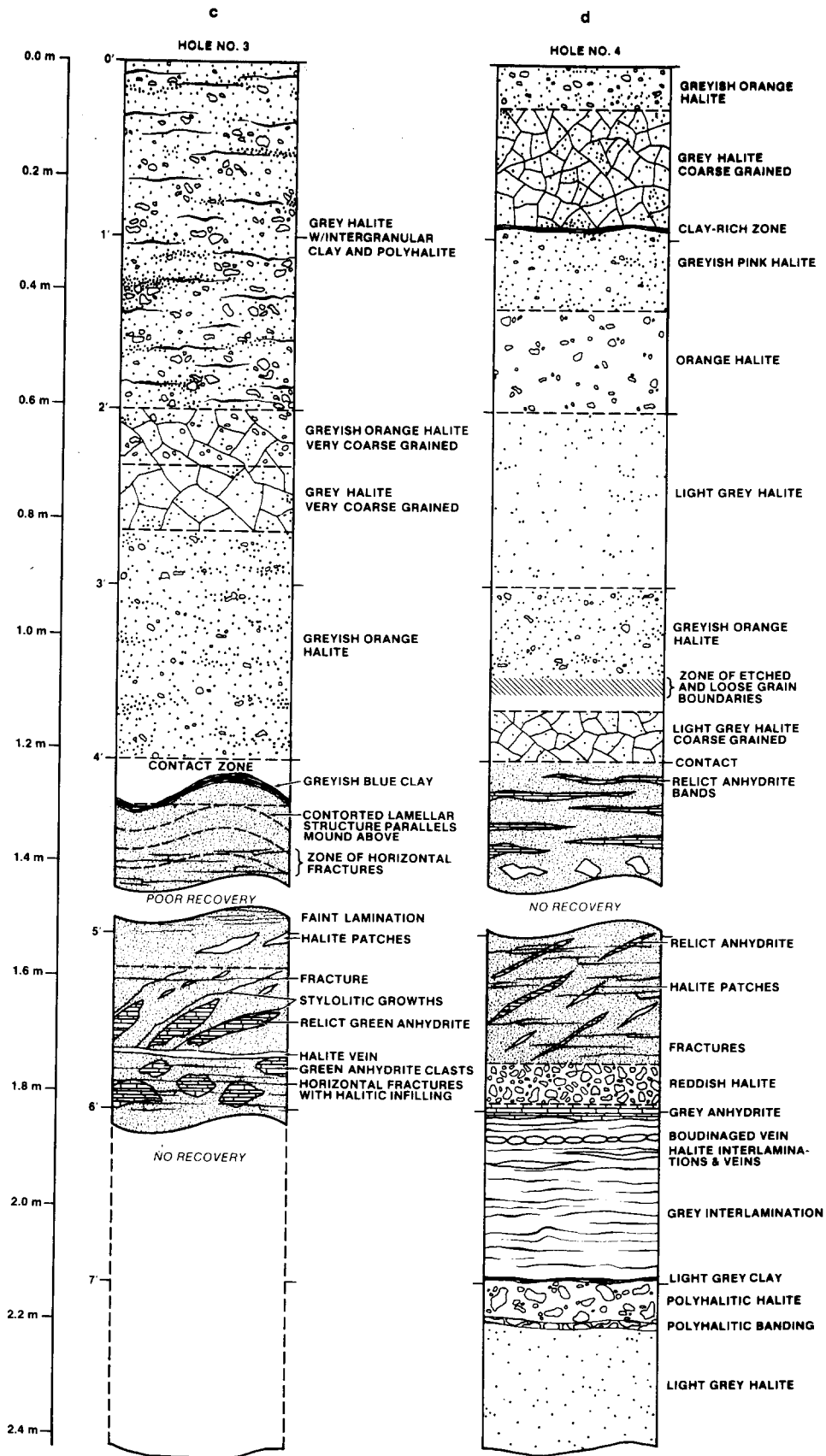


Figure 4. (Continued)

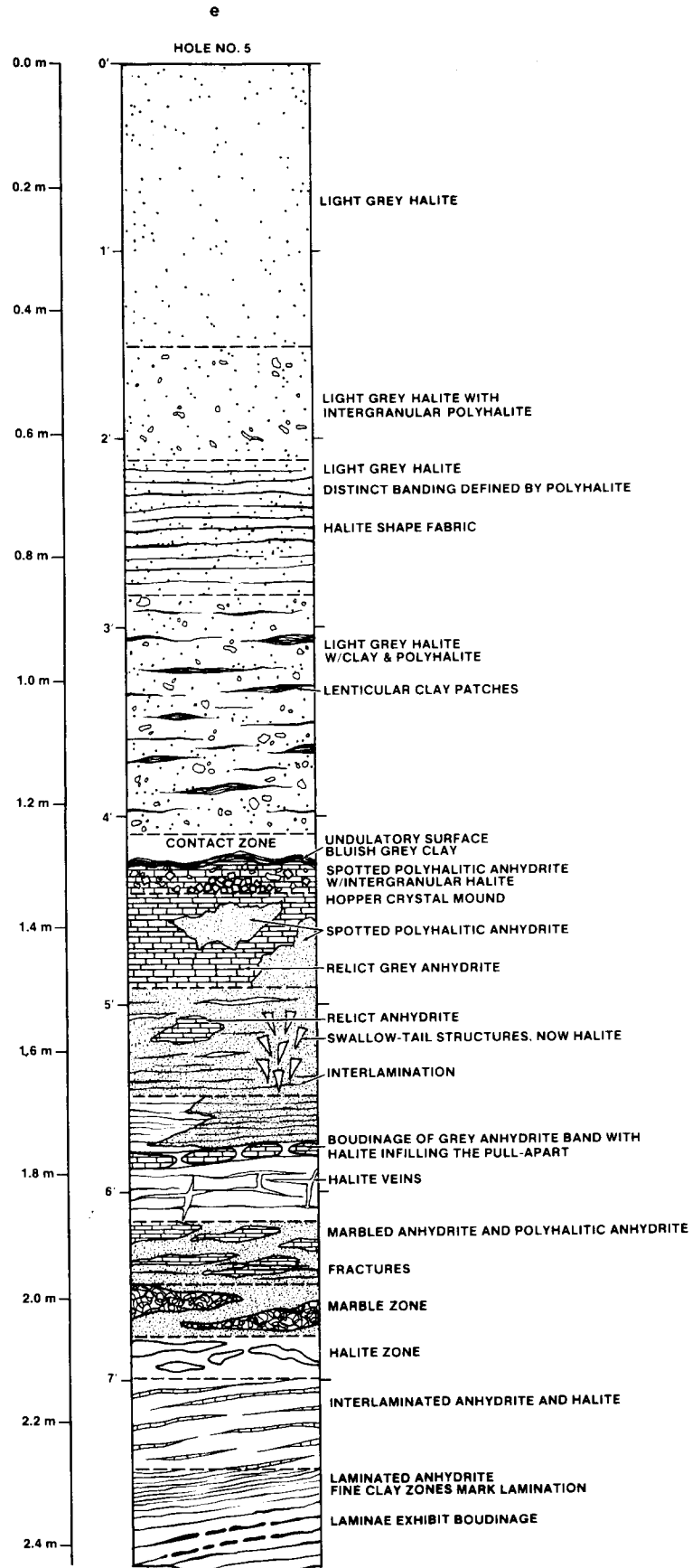


Figure 4. (Concluded)

The **Upper Contact Zone I** displays complex structure and mineralogy. The zone includes a distinctive claystone up to several centimeters thick in which are observed the major undulation structures of interest within MB139. The claystone occurs primarily along the undulatory upper contact of Zone I, with the polyhalitic halite above. The undulations along the upper surface of MB139 are 10 to 50 cm in amplitude and 30 to 100 cm in wavelength. The lower portion of this zone is not as regular in form and content as is the upper portion. Where Zone I is thin and the claystone is in contact with the polyhalitic anhydrite of Zone II (see description below), the claystone infills embayments into the anhydrite. The distinct lower portion of Zone I is absent. Also, the contact or transition between the lower portion of Zone I and the upper portion of Zone II can be indistinct. Where it is, the lower portion of Zone I consists of interlayered halite, polyhalite, and clay. These interlaminated zones thicken in the areas beneath the upper surface undulations. Within these undulations, clusters of hopper crystals are observed partially broken up but preserving their distinctive texture. They are incorporated within the laminae of halite, polyhalite, and clay. Such textures are probably equivalent to the "crushed crystals" of Jarolimek et al. In a 36-in.-dia hole in Room 4, an undulation with an amplitude of ~0.5 m was intersected. On the limb of this undulation, a fracture crosscuts Zone I, terminating horizontally in the stratigraphically lower Zone II (see description below) and higher halite.

The **Massive Polyhalitic Anhydrite Zone II** lies immediately below the claystone or interlaminated portion of Zone I. The zone is 20 to 30 cm thick. Relict grey-green patches of anhydrite are found in this zone with embayed margins where a red polyhalitic anhydrite overprints the relict anhydrite. A distinct spotted appearance characterizes this polyhalitic anhydrite. These spots are 1 to 5 mm in diameter and are formed from radiating clusters of polyhalite. Contorted and undulated stylolitic laminae are observed and crosscut both anhydrite and polyhalitic anhydrite. Some boreholes in this zone reveal clusters of swallowtail structures and replacement patches of halite.

The **Mixed Anhydrite and Polyhalitic Anhydrite Zone III** has a distinct marbled appearance enhanced by the mixture of red and green colors. The colors reflect patches of relict grey-green anhydrite and reddish polyhalitic anhydrite. This zone (as is Zone II) is 20 to 30 cm thick; its appearance suggests a relict breccia that has been overgrown by secondary minerals. In this zone, a pervasive set of subhorizontal fractures is observed. These fractures are partially infilled with halite and polyhalite, but a porosity

remains, probably interconnected within the fracture trace. Some of the relict green anhydrite patches exhibit brecciation and pullapart or boudinage deformation. Halite occurs as veins and secondary replacement patches. Relict anhydrite patches and stylolitic laminations in some boreholes dip $>25^\circ$.

The **Laminated Anhydrite with Halite Zone IV** is characterized by fine laminations of halite and grey-green relict anhydrite. This zone of laminae is 20 to 30 cm thick. Individual subhorizontal laminae are 1 to 2 cm thick. The distinctive red-orange color, derived from polyhalite (which overprints anhydrite in the section above), is absent. Anhydrite occurs either as a multiple laminae with thin (<1 mm) interlaminae of clay or as laminae in halite. Anhydrite laminae in halite exhibit pullapart structures (boudinage) and crenulations, but the undulose structures of Zone I and structures as displayed by the stylolitic laminae in Zone II are not observed in this zone. Also, subhorizontal fractures continue in this zone. As in Zone III, such fractures are infilled partially by halite. The fractures in this zone are similar in orientation and content to the fractures in the zones above, but no high-angle fractures have been observed that interconnect between zones. Thicker bands of halite (2 to 5 cm) are observed in the zone, but such bands cannot be traced hole-to-hole.

The **Lower Contact Zone V** is marked by a grey-blue clay zone. Much of the clay is often lost during drilling, but where the section is recovered intact, the clay band appears to be 1 to 2 cm thick. While the upper surface of the clay zone is largely conformable to the structures in MB139, the clay band along the lower surface infills embayments in the salt unit below. These embayments are 1 to 5 cm deep and 1 to 5 cm wide. There is also a gentle undulation of the Lower Contact Zone with a wavelength of 75 cm and an amplitude of 10 cm. No undulations were observed similar to those encountered within the Upper Contact Zone.

Bounding Halite Units

The halite units above and below MB139 are characterized by coarse-grain intergranular polyhalite and clay. A color lamination is distinctive in both halite units, but more so in the halites above MB139. The color is imparted by the dominant intergranular mineral: halite is pale grey if the dominant mineral is clay and is red-orange if polyhalite is the dominant mineral. The color bands are 15 to 30 cm thick. Portions of these units contain many mesoscopic fluid inclusions. Some isolated clay seams (≤ 1 cm) are observed. These clay seams and the color-banding impart a sense of horizontal layering in the salt units.

Discussion of the Origin of Undulations on the Upper Surface of MB139

The origin of the undulations along the upper surface of MB139 was the original question by the EEG of the State of New Mexico that sparked this study of the marker bed. The EEG's major concern was whether these observed structures evidence a deformational event that postdates deposition and diagenesis of the facility interval and that affects the facility level. The following processes can be envisaged for forming the undulations:

- The growth of gypsum that forms the undulations by
 - Differential growth rates between surfaces on which gypsum swallowtails are and are not forming
 - "Force of crystallization" that deforms the host rock as a result of the stress applied by the growth of the new mineral (gypsum) within the host (anhydrite)
 - The volume change associated with altering anhydrite to gypsum and vice versa
- Local response to the growth of larger scale structures in the Castile Formation, 200 to 300 m below MB139
- Deformation associated with the environments of deposition and diagenesis. Examples are soft-sediment slumping, erosion and resedimentation (often through traction deposition), and dewatering.

Mechanisms Involving Gypsum Growth—Several authors have suggested multiple mechanisms related to the growth of gypsum that may produce deformation in evaporite sequences (see above list). Jarolimek et al suggested the syndepositional growth of gypsum as a mechanism for undulation growth. Such growth is observed in the swallowtail structures of MB139. The wording of the Jarolimek et al report is ambiguous as to whether the mechanism is the force of crystallization during gypsum growth or whether it is the different rates of growth between surfaces where gypsum swallowtails do or do not grow. Powers (1984) indicates that the mechanism of different growth rates was the intended mechanism in the earlier report. In detail, Powers suggests a mechanism:

... the swallowtail mounds were basically growing on the underlying sediment into the water column, not jacking up the overlying sedi-

ment ... Precipitation [of anhydrite or polyhalitic anhydrite, author] did not keep pace with gypsum growth ... halite then precipitated which filled in the lows.

This mechanism is feasible but inconsistent with direct observation of MB139. If differential growth rates occur, the areas of swallowtail growth should correspond to undulations above them. At least in holes of Room 4, no correlation exists between the presence of swallowtail growth and undulations above the swallowtails (Figure 4). Also, the small-scale structures of gypsum crystals in MB139 indicate that their growth did not create the observed undulations. As these gypsum crystals grow, they form subhorizontal laminae (Figure 5). Several of these laminae may be stacked on top of each other; however, the growth of the lower band does not distort the band above. Also, the individual gypsum crystals contain subhorizontal laminae of anhydrite, which represent slight shifts of the stable phase in response to fluctuations of fluid concentrations during formation. These laminae, which can be traced across the band of gypsum crystals without significant displacement, suggest uniform growth rates along the growing surface and indicate that anhydrite was precipitating concurrently and keeping pace with the growth of the gypsum crystals in the swallowtail structure.

The other inferred mechanism, the force of crystallization, requires these elongate grains in the swallowtail structures to act as "jacks" that physically displace the overlying sediment during growth. This mechanism of forming undulations by the growth of swallowtail gypsum can be discounted by several arguments. One, an old concept of "the force of crystallization," is resurrected for the growing gypsum crystal to deform the overlying sediment. This concept was once put forward as the driving mechanism for large-scale tectonic deformation. For mechanical and textural considerations it is no longer a favored mechanism for rock deformation. Basically, a crystal grows to minimize free energy. Surface free energy, nucleation steps, and the orientation of the stress axes are important parameters in this growth and its orientation. Observation, theory, and experiments suggest that crystals grow elongate parallel to the axes of minimum stress. Such growth involves mass transfer through paired reactions, or nearly one-to-one replacement of the preexisting matrix. Hence, mass and volume in the entire rock system are not significantly changed except for change in geometry, fluid loss, and the outward transport of chemical species in the evolving fluid. In short, crystals will not grow against the maximum stress as required if the "force of crystallization" were the undulation-forming mechanism.

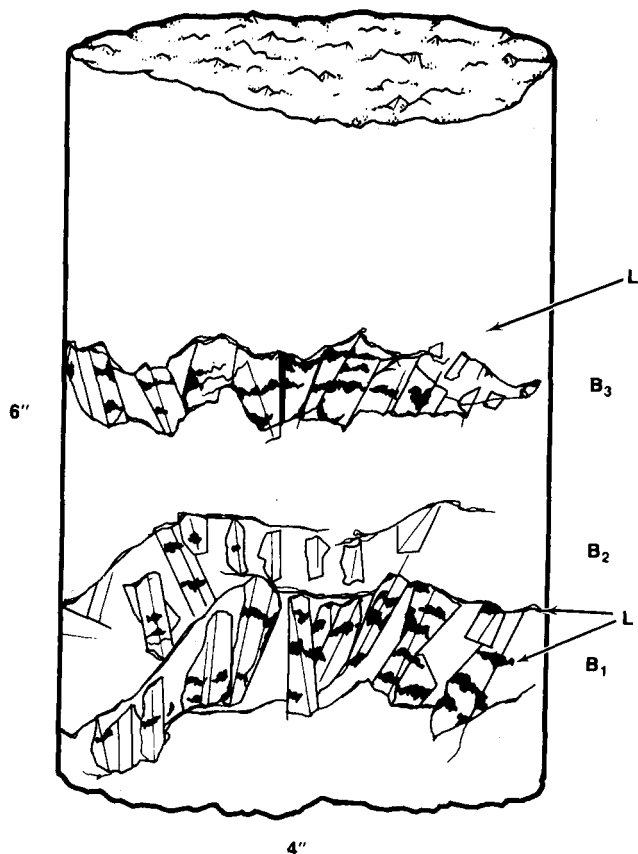


Figure 5. Multiple partial or complete bands, B1 to B3, of swallowtail growth in Hole 5, 5 ft, in which the adjacent bands are not contorted harmonically. (Therefore, deformation of the bands did not accompany the new growth stage of gypsum. Also shown are laminae (L, solid black) internal to a swallowtail crystal. These laminae can be traced from crystal to crystal and represent temporary shifts back to anhydrite precipitation from gypsum growth during the growth of the swallowtail.)

Mechanisms Involving Salado Response to Castile Deformation—The possible connection between the MB139 undulations and the anti- and synforms* in the underlying Castile Formation needs careful consideration since this is one of the major concerns of the EEG. Jarolimek et al concluded that the only evidence for a tectonic or gravitational deformation in MB139 was the clusters of “crushed” halite grains in the core of some undulations. They interpreted these to represent the effects of the accumulating overburden. This study basically concurs with the observations of Jarolimek et al that the laminar markers in the MB139 interval do not exhibit undulations similar to those in the upper contact zone of the marker bed, either in terms of spatial association or in terms of scale. As a result of the viscosity contrasts between

*Considered to be gravitational in origin (Borns et al, 1983)

halite and anhydrite, a thin anhydrite layer can be folded while the laminar markers in the host halite may remain relatively planar through compensating flow at scales larger than microscopic and grain size scale. Therefore, the planar nature of such laminae in the host halite cannot preclude the occurrence of a larger scale deformational event affecting the rock mass and in isolated folding of the anhydrite layer. However, the lack of undulations in zones internal to the marker bed sequence, such as Zone IV and Lower Contact Zone V of MB139, indicates that the marker bed was not folded as one unit and that the undulations are not part of a penetrative deformation of the lower Salado.

This limited stratigraphic distribution of undulose structures associated with MB139 narrows the possible age range in which the undulations formed. The lack of penetrative structures, other than fractures crosscutting halite and anhydrite at the upper undulatory contact of MB139 above and below the marker bed, suggests that the undulations formed during deposition and that the process possibly extended into the diagenesis of the unit. Also, the process that formed the undulations was not active during accumulation of the units above and below the marker bed. This time frame is also inferred from structures such as clusters of hopper crystals described below.

Mechanisms Related to Deposition and Diagenesis—Evaporite sequences such as the Salado form in complex environments (Handford and Bassett, 1982). For any given unit, its deposition may be part sub-aerial or part submarine at any given time. These environments oscillate, and the process of transition may result in the structures observable in MB139. Key structures can be observed in the units, which fingerprint processes that formed the undulations. In some boreholes, the cores of the undulations are accumulations of hopper crystals (Holes 2 and 5, Figure 4). These hopper crystals are apparently the structure that Jarolimek et al interpreted as “crushed” crystals. These clusters of hopper crystals (Figure 6) are a significant clue to the processes active during formation of the undulations. As stated in the introduction, several workers believe that the Salado represents cycles of desiccation and submergence (Handford et al, 1982). MB139 displays one of these cycles, although the transition may be abrupt. The formation of the relatively thick unit of anhydrite and associated minerals indicates a desiccation cycle. By the time the massive polyhalitic anhydrite (in Zone II) formed in accord with this scenario, Zone II was covered by very shallow water or incompletely covered with shallow

pools, and the substrate may already have been deformed by soft-sediment slumping or by current reworking of the upper portion of the deposit. In the shallow pools, hopper crystals of halite were forming. Another Salado cycle commenced with submergence, either through flooding of the mudflat and salt-pan environment or through a rising sea level in the intertidal or shelf margin region. Such an increase in water level and fluid flux often accompanied high-energy processes such as flooding or wavebase reworking of sediment, which was deposited in a quiescent environment. In these high-energy environments, the hopper crystals were swept up and accumulated in traction* deposits or by wave-ripple deposits also described by Lowenstein (1982).

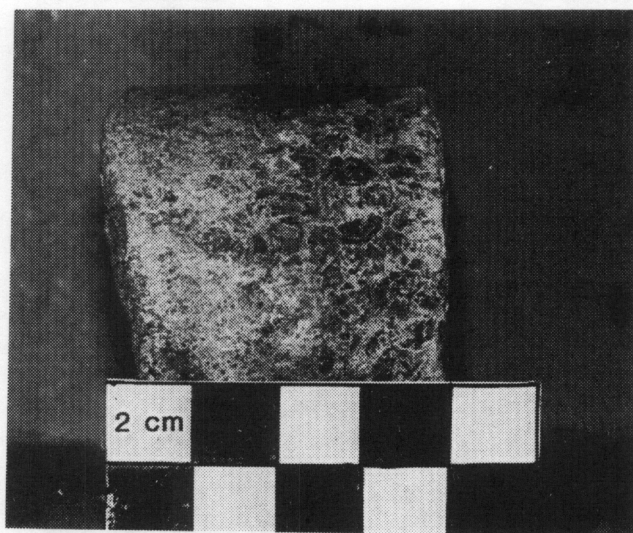
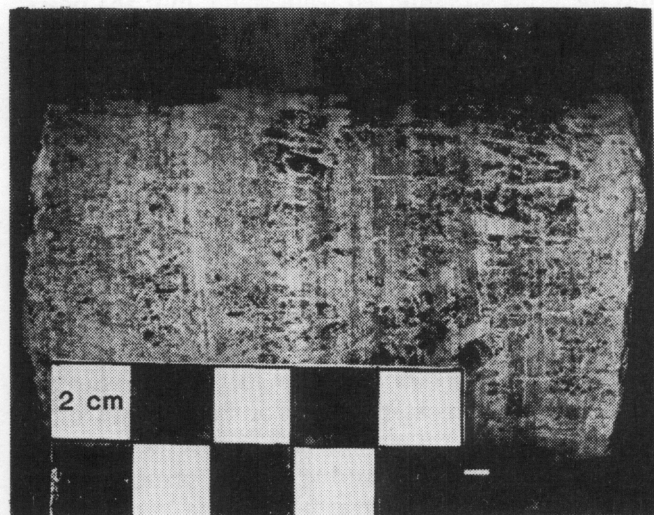


Figure 6. Accumulation of hopper crystals within the Upper Contact Zone I of MB139, with intergranular polyhalite and secondary veining (Room 4, Hole 5, 4.1 to 4.4 ft)

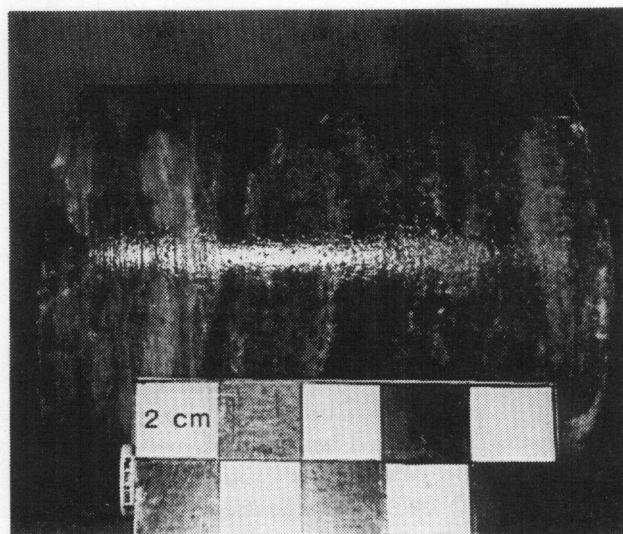
These depositional environments are also suggested by the distinct gypsum growth structures evident in the MB139 section ranging from spectacular swallowtail arrays to crystals 1 mm to 1 cm long that formed perpendicular to the stratification (Figure 7). Gypsum was replaced in these structures by halite and anhydrite. Identifying the gypsum is based on the relict morphology exhibited in the pseudomorphs. These gypsum textures are interpreted by several workers; e.g., Handford and Bassett (1982) and Lowenstein (1982), as the result of subaqueous growth in shallow evaporative lagoons associated with ephemeral salt-pans. The formation of the crystals in a swallowtail structure is therefore syndepositional. This syndepositional growth is also suggested by the

*"Traction" as used in this report means the transport and reworking of sediment by current flow at the sediment-water interface.

fine laminae included in the gypsum grain and composed of either clay or anhydrite. These laminae can be traced continuously through several pseudomorphs (Lowenstein, 1982). Similar textures observed in MB139 represent the growth stages of the gypsum crystal through cycles of precipitation and dissolution or erosion. The continuity of these dissolution laminae from one swallowtail to another along the band suggests similar rates of growth along the band.



(a) Swallowtail growth structures after gypsum in Zone II. (Gypsum is now replaced by halite; the groundmass is polyhalitic anhydrite; and the anhydrite is faintly laminated; Room 4, Hole 5, 5 ft.)



(b) Marbled nature of mixed anhydrite and polyhalitic anhydrite in Zone III. (Light-colored anhydrite bands have nodular to enterolithic appearance; Room 4, Hole 5, 6.5 ft.)

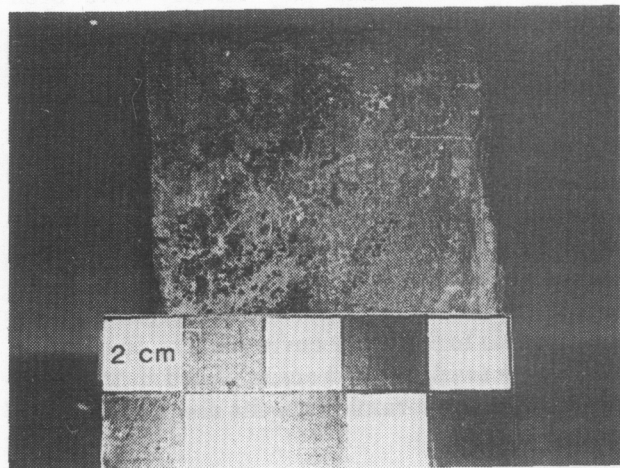
Figure 7. Gypsum growth structure evident in the MB139 section

This inference of uniform rates counters the argument that a more rapid growth in regions of swallow-tail development created the undulations, as proposed by Jarolimek et al.

These specific structures—gypsum swallowtails and redeposited hopper crystals—do not specifically define the mechanism that formed the undulations in the upper portion of MB139. However, the structures and the processes inferred from them limit the possible environments. Such undulations can be inferred to have formed in an intermittently shallow water environment such as the intertidal zone or a salt-pan. Undulations could form through wave action or through transient action of channels in the salt-pan and mudflat environments. The minimal amount of exposure produced by drilling and mining in the WIPP facility does not yet permit a choice between these processes.

Other structures developed in the marker bed in addition to the undulations. In Zones I through III, some laminar markers are inclined $\sim 45^\circ$ (Figures 4 and 8) and are truncated upward and downward within the marker bed. This may indicate some repeated soft-sediment slumping during deposition of the unit. Other processes are suggested by the presence of crenulated stylolitic laminae and pullaparts of anhydrite laminae (Figure 9). These structures are not clearly syndepositional. The stylolitic laminae may reflect water loss during diagenesis and the effects of inhomogeneous bulk flattening on the unit during continued sedimentation, compaction, and diagenesis. The pullapart structures in anhydrite laminae may result from the same increase in overburden and resultant flattening. Yet it remains unclear on textural evidence as to when these pullaparts formed in a relative time scale, except that they predate the subhorizontal fractures crosscutting the pullaparts and other structures such as stylolitic laminae.

The Origin of Fractures in MB139—The subhorizontal fractures probably characterize the postdiagenetic deformation of the anhydrite units in the Salado. The other structures described in the preceding paragraphs, including inclined markers, have a ductile appearance and probably reflect the rheological behavior of the unit before lithification. A brittle response would be expected of anhydrite after diagenesis under the limited stresses and temperatures of the middle Salado. Still, note that the ductile behavior may occur in response to gravity-driven deformation of anhydrite units of the underlying Castile Formation under postulated stresses and temperatures that would also favor brittle behavior (Borns et al, 1983). The apparent contradiction between theory and field



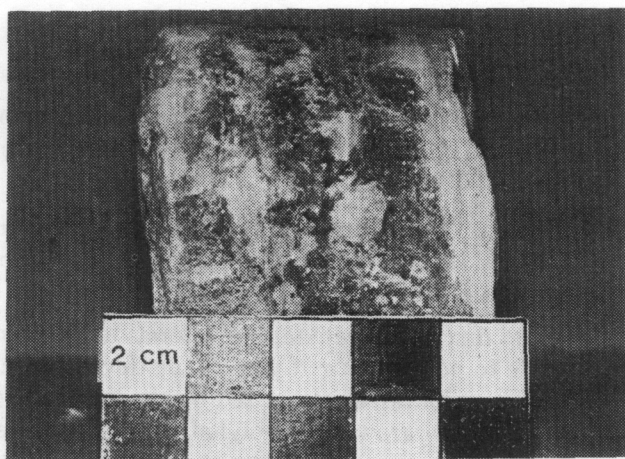
(a) Inclined polyhalitic anhydrite and halite lamination of Zone II. (Dipping structures extend into more polyhalitic section to the right; spotted appearance is beginning to be distinctive; Room 4, Hole 5, 4.6 ft.)



(b) Inclined lamination in Zone II. (Laminae are polyhalitic anhydrite and halite. Polyhalite overgrows halite and anhydrite with distinctive spotted appearance; Room 4, Hole 5, 4.6 ft.)

Figure 8. Inclined laminations in Zones I through III

observation is partly a result of not considering the effects of intergranular fluids and of different mineral mixtures for the evaporite units. The significant observation about the fractures in Zone III is that they are predominantly subhorizontal ($>90\%$) and are partially infilled. The partially infilled nature indicates that these fractures were not formed after excavation of the facility, although their current configuration may be modified by the excavation. The orientation suggests a consistent orientation of the stress field at the time of fracture formation. The textures suggest that fracturing occurred between deposition and excavation. Only a few processes could have produced these fractures:



(a) Laminated anhydrite and halite in Zone IV. (Pullapart and deformation are exhibited in some anhydrite bands; other bands are intact; Room 4, Hole 4.)



(b) Pullaparts of markedly discontinuous anhydrite bands in Zone IV; Room 4, Hole 4

Figure 9. Crenulated stylolitic laminae and pullaparts of anhydrite laminae in Zone IV

- Stresses that developed in the Salado and were generated by deformation in the underlying Castile Formation, such as gentle buckling of the Salado over a Castile anticline
- Changes in the overburden pressure coupled to sedimentation and erosion cycles affecting the rock sequence above the marker bed
- Buildup of gas pressures within the unit as a result of decomposition of organic material, whether algal or bacterial

The deformation of the underlying Castile Formation is characterized by synforms and antiforms. In some forms of cylindrical folds, the stress vectors are such that horizontal fractures are expected near the inflection point of the limb at most scales (Dietrich,

1970). The fractures of MB139 may reflect such a region. However, across the form of the fold the orientation of the stress axes changes, and nonhorizontal fractures should form. The uniform orientation of the fracture system in MB139 is not consistent with that expected for a system connected to Castile deformation. This conclusion is limited by the areal distribution of observations to date on fracture orientations in MB139.

The height of the sedimentary section that existed above the WIPP facility horizon at different stages in the geological history is a significant variable, although not well-quantified. Extrapolation of the stratigraphic data in Powers et al (1978) suggests that as much as double the current thickness of overburden may have existed. Also, this overburden formed and diminished in cycles after the Permian (Figure 10). The drops in overburden were rapid. These cycles may have produced the stress relief and orientation of stress axes to account for the observed system of subhorizontal fractures in MB139. Once the fractures opened, the available fluids in the unit flowed into the fractures down the induced pressure gradient. The halite and polyhalite infilling the fractures formed from these fluids.

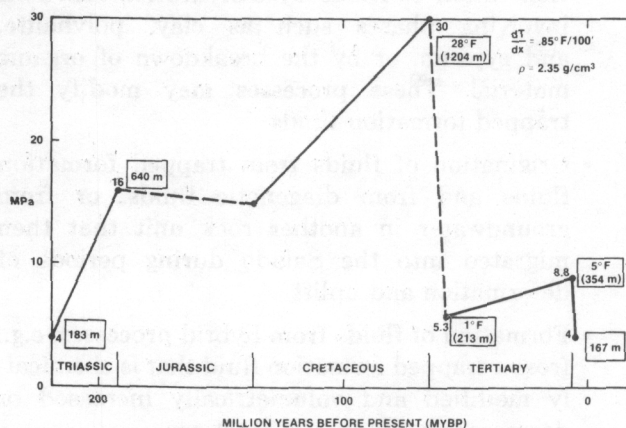


Figure 10. Overburden from the Permian to the present above the Rustler-Dewey Lake contact, which is the highest major marker without effects of post-Permian erosion. (Therefore, the interval thicknesses from the Rustler-Dewey Lake contact and units below are relatively constant. The overburden increment for these constant intervals such as between the contact and the facility horizon can be derived from the interval length; e.g., Rustler-Dewey Lake contact to the facility horizon (1600 ft, 12 MPa). The total overburden can be calculated by summing the value for the time of interest from the figure and the constant value calculated for the interval of interest. The overburden is expressed in MPa. The temperature increment with depth of burial since the Cretaceous is shown in boxes and is derived from temperature profile for drillhole AEC 8 (Mansure and Reiter, 1977). The overburden was calculated by assuming a sandstone density of 2.35 g/cm³ and by using the range of overburden depths derived from Powers et al (1978).)

The concept that gas pressures build up in response to organic decomposition is difficult to evaluate but requires consideration. The problem hinges on whether enough organics are present in the unit and on the rates at which the gas is produced. Also, the gas permeabilities in the unit may be large enough relative to liquid permeabilities to preclude the build-up of gas pressures high enough to initiate hydrofracturing. In summary, no compelling evidence exists that disseminated organics produced an in situ build-up of gas as a result of decomposition within MB139, but neither do observations contradict this mechanism as the origin of gas buildup.

Origin of Fluids Associated With MB139—The meso- and microscopic textures observed in MB139 suggest some possible mechanisms for the origin and modes of accumulation for the fluids associated with MB139. Possible sources for these fluids follow:

- Trapping of formation fluids along grain boundaries or in fluid inclusions since diagenesis
- Generation of fluids by dehydration reactions involving phases such as clay, polyhalite, and gypsum, or by the breakdown of organic material. These processes may modify the trapped formation fluids
- Origination of fluids from trapped formation fluids and from diagenetic fluids, or from groundwater in another rock unit that then migrated into the Salado during periods of deformation and uplift
- Formation of fluids from hybrid processes; e.g., from a trapped formation fluid that is chemically modified and volumetrically increased or decreased by diagenetic reactions

Further investigations of the chemical composition and the hydrologic characterization of the brine encounters will reveal which source is plausible. Preliminary work on the compositions of the brines in conjunction with analysis of fluid inclusion composition suggests that the brines of the facility horizon did not directly originate as fluid inclusions (Stein, 1984). Hence, except for eliminating some sources such as fluid inclusions, we cannot yet isolate the origin of the fluids. At best we can only identify sources as stated above that are consistent with the reconstructed envi-

ronment and with the history of the interval. Several stages of fluid flux can be inferred from the textures present in MB139:

- Dewatering associated with compaction and diagenesis, as suggested by the development of stylolitic textures.
- Fluid flux accompanying the alteration of anhydrite to polyhalite and postdating development of the stylolites, as suggested by the patchy and spotted overgrowths of polyhalite on anhydrite. These overgrowths crosscut the stylolitic structures.
- A younger stage of fluid flux, as observed in the subhorizontal fractures with the partial infillings of polyhalite and halite. These fractures crosscut the polyhalite overgrowths and the stylolitic structures.

These observations indicate the presence of fluids throughout the history of MB139—fluids that were able to migrate either along fractures or along grain boundaries. These fluids (or their daughters) are probably present today. If these fluids are dispersed in the rock mass, then certain processes can concentrate them:

- Migration of fluids from fluid inclusions or grain-boundary films in halite to a reservoir that is either a clay seam or a fractured anhydrite. This migration is driven by stress or by thermal gradients.
- Flow from clay zones above and below the anhydrite into the anhydrite when the mine is excavated; fracturing occurs during creep. These zones are permeable and have accepted fluid.
- Development of fractures in anhydrite during its postdepositional history. Fluid migration is driven down pressure gradients. Clays, which are impermeable relative to fractured anhydrite, act as a seal. The relative permeabilities of the clay zones in this scenario and the one above are contradictory; e.g., clays in this scenario are the seal, whereas in the scenario above the clays are water-bearing. The difference between the two scenarios is that this one includes the effects of fractures within the anhydritic units.

Conclusions

1. Several distinctive structures are exhibited in MB139:
 - The undulations in the Upper Contact Zone I were the original focus of this study and of preceding studies. These undulations are marked by bands of claystone, halite, and polyhalite. Their cores exhibit clusters of hopper crystals in some structures, and their amplitude and wavelength are highly variable.
 - Distinct from the Zone I structures above, contorted and undulated textures are observed in Zones II and III. Stylolytic laminae are the most characteristic feature. Highly inclined laminae are also observed. No strong correlation in orientation exists between these structures and the undulations in Zone I above. Variations in thickness for Zone II may be associated with the undulations in Zone I in that the thinning of Zone II may reflect erosion during the submergence cycle that began with the formation of Zone I.
 - Anhydritic laminae in Zone III and distinctly in Zone IV where the anhydrite and halite are interlaminated show pullapart structures. The sense of extension is horizontal, although some crenulation of the horizontal laminae is observed.
 - Horizontal fractures are a distinctive feature of Zone III, but they also extend in some holes into Zones I or III. In one hole a fracture can be traced across the upper contact of MB139. Generally, these fractures are partially infilled with polyhalite and halite; an interconnected porosity remains. The fractures also crosscut all the structures described above.
2. MB139 represents a period of intermittently shallow water deposition in the cycles of desiccation and flooding that characterize the Salado. The varied growth textures of halite (e.g., hopper crystals and swallowtail structures) are evidence of these environments. The irregular upper surface was created as traction deposits by a sedimentary reworking of unconsolidated sediments in the upper zones of MB139. This reworking probably relates to the stage of submergence that terminated deposition of the marker bed. This process is indicated by the cores of hopper crystals within the undulations.
3. The conclusion above suggests an origin for the undulations other than a deformational event after deposition of MB139. However, the sub-horizontal fractures that are common to the marker bed represent a deformational event. The effects of these fractures on fluid flow and entrapment are a significant secondary consideration for site evaluation. The fractures may represent the manifestation in the Salado of the gravity-driven deformation seen within the underlying Castile or of sedimentation-denudation cycles occurring after deposition of the repository interval. The extent to which Castile deformation influences the Salado awaits programs such as analyzing the DOE-2 core and physically modeling the gravity structures by centrifuge. To date, such effects in the Salado have not been reported except in the DOE-2 area.
4. Secondary structures and effects of minor deformational events such as regional uplift are important factors in characterizing MB139 because these features provide reservoirs for fluids and zones of enhanced permeability. For example, the accumulation of an overburden that was almost double the current overburden combined with rapid denudation also induces fracturing. The horizontal orientation of fractures in MB139 appears to favor this latter mechanism. Fluids, both past and present, are important parts of any discussion of MB139. Several drillholes and close excavations near or through MB139 have produced fluids. The local source of these fluids is probably the partially open fractures in the marker bed, not the bounding clay seams. Determination of the size and interconnectivity of these reservoirs awaits the results of ongoing studies. The primary origin of these fluids is under investigation by C. Stein and J. Krummhansl of Sandia National Laboratories and by J. Morse of the Technical Service Contractor. Preliminary results suggest different compositions for MB139 fluids than for fluid inclusions from halites in the same facility interval as MB139. Hence, the MB139 fluids do not originate directly from inclusion migration.
5. The halite patches (which replace groundmass anhydrite) and halite pseudomorphs after gypsum, together with the polyhalite overgrowths, suggest stages of fluid flux through the marker bed after deposition. The fractures partially filled with halite or polyhalite also indicate

that some of this fluid flux occurred after consolidation. Hence, fluids have been associated with and have interacted with the marker bed throughout its history. Similar marker beds in the Salado may exhibit similar histories.

6. The MB139 represents a complex history of depositional and postdepositional events. The fractures, the cyclic stress history, and the internal stratigraphy of the marker bed show that the unit is not a simple anhydrite beam. Future studies of, and models of, the WIPP facility horizon need to account for these complexities. Also, the Salado units at the WIPP site are not strictly static at present. They have rapidly denuded in the last 10 my, and the horizontal fracture sets may represent the continued readjustment of stresses within the evaporitic units accompanying this dynamic system.

References

- D. J. Borns et al, *Deformation of Evaporites Near the Waste Isolation Pilot Plant (WIPP) Site*, SAND82-1069 (Albuquerque, NM: Sandia National Laboratories, March 1983).
- W. E. Dean and B. S. Schreiber, eds, *Marine Evaporites, Lecture Notes for Short Course No. 4*, Oklahoma City, April 1978, Society of Economic Paleontologists and Mineralogists, Tulsa, OK (1978).
- J. H. Dieterich, "Computer Experiments on Mechanics of Finite Amplitude Folds," *Canadian J of Earth Sciences*, 7:467-476 (1970).
- C. R. Handford and R. L. Bassett, "Permian Facies Sequences and Evaporite Depositional Styles, Texas Panhandle," in C. R. Handford, R. G. Loucks, and G. R. Davies, eds, *Depositional and Diagenetic Spectra of Evaporites - A Core Workshop*, SEPM Core Workshop No. 3, Calgary, Canada (1982).
- C. R. Handford, R. G. Loucks, and G. R. Davies, eds, *Depositional and Diagenetic Spectra of Evaporites - A Core Workshop*, SEPM Core Workshop, No. 3, Calgary, Canada (1982).
- L. A. Hardie and H. P. Eugster, "The Depositional Environment of Marine Evaporites: A Case for Shallow Clastic Accumulation," *Sedimentology*, 16:187-220 (1971).
- L. Jaroloimek, M. J. Timmer, and D. W. Powers, *Correlation of Drillhole and Shaft Logs, Waste Isolation Pilot Plant (WIPP) Project, Southeastern New Mexico, Report #TME 3179* (Albuquerque, NM: US Department of Energy, 1983).
- C. L. Jones, C. G. Bowles, and K. G. Bell, *Experimental Drill Hole Logging in Potash Deposits of the Carlsbad District, New Mexico*, USGS Open File Report 60-84 (1960).
- C. L. Jones and B. M. Madsen, *Evaporite Geology of the Fifth Ore Zone, Carlsbad District, Southeastern New Mexico*, USGS Bulletin 1252-B (1968).
- T. Lowenstein, "Primary Features in a Potash Evaporite Deposit, the Permian Salado Formation of West Texas and New Mexico," in C. R. Handford, R. G. Loucks, and G. R. Davies, eds, *Depositional and Diagenetic Spectra of Evaporites - A Core Workshop*, SEPM Core Workshop No. 3, Calgary, Canada (1982).
- A. Mansure and M. Reiter, *An Accurate Equilibrium Temperature Log in AEC No. 8, A Drill Test in the Vicinity of the Proposed Carlsbad Disposal Site*, NM Bur of Mines and Mineral Resources, Open File Report No. 80 (1977).
- R. Popielak, D'Appolonia Consulting Engineers, to D. K. Shukla, et al, D'Appolonia Consulting Engineers, "Gas Testing Program, Phase I, Task II," May 9, 1983.
- D. W. Powers, S. J. Lambert, S. E. Shaffer, L. R. Hill, and W. D. Weart, eds, *Geological Characterization Report, Waste Isolation Pilot Plant (WIPP) Site, Southeastern New Mexico*, SAND78-1596, Vols 1 and 2 (Albuquerque, NM: Sandia National Laboratories, 1978).
- D. W. Powers, Sandia National Laboratories, personal communication, 1984.
- C. L. Stein, Sandia National Laboratories, personal communication, 1984.

APPENDIX

Mesoscopic Description of MB139 Core From The Five-Hole Array in Room 4

<u>Depth (ft)</u>		<u>Core Description</u>
<u>From</u>	<u>To</u>	
Hole No. 1, Box No. 1		
0.0	0.5	No recovery
0.5	1.6	Halite, very light brownish-grey (5YR7/1); very coarse grain size (1 to 2 cm in diameter), triple-point grain boundary configuration. Intergranular clay (~2%), bluish-grey (5B6/1). Clay also occurs as intergranular patches 0.5 cm in diameter; light-brown intergranular staining (5YR5/6). Many 1- to 2-mm-wide separations (at 0.7, 1.3, 1.5 ft)
1.6	2.1	Halite, pale greyish-orange (10YR8/4); very coarse grain size. Intergranular clay, medium bluish grey (5B6/1). Clay is <2% of rock. Intergranular hematitic staining, moderate reddish-orange to brown (10R6/6-10R4/6). This staining imparts the dominant color of the halite and leads to the color change in the halite unit. Weak trace of horizontal lamination. Many 1-to 3-mm dia fluid inclusions
2.1	2.25	Halite, greyish-orange to pink (10R8/4); 3% intergranular hematitic staining, moderate reddish-brown (10R4/6). Many horizontal partial separations; one planar clay band, medium bluish-grey (5B6/1)
2.25	3.5	Halite, pale reddish-brown and dark reddish-brown (10R5/4 to 10R6/6). Intergranular hematitic staining, moderate reddish-brown (10R6/6). Staining is ~2% of rock. Many fluid inclusions 1 to 3 mm in diameter
Hole No. 1, Box No. 2		
3.5	3.9	Halite, pale pinkish-grey (5YR8/1); very coarse grain size, good equilibrium mosaic; 3% intergranular polyhalite, moderate reddish orange (10R6/6). Intergranular clay patches, 1 cm wide on horizontal surfaces. Many horizontal partial separations; many fluid inclusions
3.9	4	Contact between the coarse-grained halite described above with finer grained polyhalite and anhydrite. Contact is undulatory (2 cm amplitude, 4 to 6 cm wavelength). A 0.5-cm-wide band of clay remains at the contact. Clay is light-to-moderate bluish-grey (5B7/1 to 5B5/1), but some portions are greenish-grey (5G6/1). Halite immediately above the contact exhibits partial separations, but the separations are not observed in the upper polyhalitic anhydrite
4	4.75	Polyhalitic anhydrite, moderate reddish-orange (10R6/6), with relict patches of anhydrite, very pale blue-green (5BG8/2), e.g. 4.1 ft. Anhydrite is overprinted by reddish polyhalitic anhydrite. The gradation between mineral types is seen by the density of reddish-orange spots (polyhalitic anhydrite), 2 mm in diameter. As spots become more dense the colors coalesce; 1- to 2-mm-wide undulatory subhorizontal stylolitic laminae, greyish reddish-orange (10R8/6). Clear halite patches that appear to be late stage. Such patches have tabular shape up to 1 cm long, with the long axes vertical and crosscutting relict blue-green anhydrite patches. These halite patches coalesce downward

<u>Depth (ft)</u>		<u>Core Description</u>
<u>From</u>	<u>To</u>	
4.75	5	Polyhalitic anhydrite, moderate reddish-brown (10R6/6). Weakly fissile, partially open fractures. Relict anhydrite patches (15%), very pale blue-green (5BG8/2). These patches impart a horizontal fabric to the rock. Halite, elongate grains, 1 cm wide and 3 to 4 cm long, tapering downward and aligned vertically
5	5.25	Polyhalitic anhydrite, moderate reddish-brown (10R6/6). Fissile, infilled horizontal fractures, pale reddish-orange (10R7/6). Some fractures are partially open; e.g., at 5.2 ft. Patches of relict blue-green anhydrite. Fractures are permeable
5.25	5.7	Core is broken up and not recovered

Hole No. 1, Box No. 3

5.7	6.4	Marbled moderate reddish-pink (10R7/6) polyhalitic anhydrite and very pale blue-green (5BG8/2) anhydrite. Many partially filled fractures; 1 to 2 mm wide, e.g., at 5.75, 5.9, 6, 6.1, 6.25, 6.35 ft
6.4	6.9	Marbled light bluish-grey (5B8/1) anhydrite, and medium olive-grey (5Y5/1) halite. Anhydrite is lenticular but also fractured and embayed. Such features are infilled with halite; some pullapart features
6.9	7	Anhydrite, light bluish-grey (5B8/1). Comminuted, 1-cm halite grains in the fractures. Intergranular polyhalite in halite veins
7	7.1	Halite-rich band, medium olive-grey (5Y5/1); medium grain size. Intergranular anhydrite
7.1	7.2	1-cm-wide light bluish-grey anhydrite laminae with 1-mm-wide greyish yellow-green (5GY7/2) interlaminae. Laminae dip at 10°. Some laminae are separated with cross-fibre halite infilling the separation
7.2	7.3	Clay-rich contact. Clay is very light bluish-grey (5B8/1). Contact with halite below MB139. Halite below the contact is pale greyish-orange (10YR8/4)
7.3	7.75	Halite, medium olive-grey (5Y5/1); coarse grain size. Coarsens downward to 1- to 2-cm-dia grains. Some finer grained sugary patches. Intergranular clay and polyhalite, although both are minor constituents
7.75	8	Halite, moderate reddish-orange (10R6/6) to moderate orange-pink (5YR8/4). Contacts between color zones are horizontal

Hole No. 2, Box No. 1

0.0	0.1	Not recovered
0.1	0.7	Halite, medium light-grey (N6); coarse grain size
0.7	1	Halite, very light grey (N8); coarse grain size, 1 to 2 cm in diameter
1	1.25	Halite, very light grey (N8); very coarse grain size, 1 to 2 cm in diameter. No preferred fabric. Intergranular polyhalite (<5%), moderate reddish-orange (10R6/6). Polyhalite blebs are <1 cm in diameter
1.25	1.75	Halite, very light grey (N8), very coarse grain size. Trace of polyhalite
1.75	2.5	Halite, light grey (N7); very coarse grain size. Intergranular blebs of polyhalite, moderate reddish-orange (10R6/6). Blebs are <1 cm in diameter and <3% of the rock
2.5	2.8	Halite, pale reddish-orange (10R6/4); coarse grain size. Horizontal partial separations, many 1-mm fluid inclusions. Polyhalite, moderate reddish-orange (10R6/6), as blebs (5 mm in diameter) in halite

<u>Depth (ft)</u>		<u>Core Description</u>
<u>From</u>	<u>To</u>	
2.8	2.9	Halite, pale reddish-orange (10R6/6); medium grain size (1 cm in diameter). Horizontal layering or separations
2.9	3.5	Halite, moderate pinkish-orange (10R7/6); coarse grain size (1 to 2 cm in diameter). Intergranular dark-grey clay (N3), <1% of the rock. Intergranular polyhalite, moderate reddish-orange (10R6/6). Halite exhibits a recrystallized mosaic. Many fluid inclusions (<1 mm in diameter). Horizontal partial separations (1 mm wide and 1 cm apart)
3.5	4	Halite, moderate reddish-orange (10R6/6); coarse grain size. Intergranular polyhalite as blebs ≤5% of the rock. Such blebs are ≤2 mm in diameter, moderate reddish-orange (10R6/6). At 3.6 ft a high-angle separation is observed that is planar along halite grain boundaries. Many horizontal partial separations
3.9	4.4	Contact of halite with MB139; partial intersection of a mound on the top surface of MB139. Contact in this segment of core is at a high angle. <i>Above contact</i> , there is halite, moderate pinkish-orange (10R7/6); coarse grain size. Intergranular polyhalite (<5% of the rock). Horizontal partial separations persist in lower halite but are truncated at contact. <i>Below contact</i> , 1- to 2-cm zone of halite and polyhalite; grain size <1 cm in diameter, moderate red (5R5/4). Interior of mound is comprised of comminuted hopper crystals of halite in matrix of greyish-pink anhydrite
4.4	4.6	Anhydrite, very pale blue-green (5BG8/2); fine grain size (<1 mm in diameter). Spotted and crosscut by polyhalite, moderate reddish-brown (10R5/2). Polyhalite forms near horizontal weak lamination that is weakly undulatory, veinlets, infilled with anhydrite (?). White (N9) veinlets have a stylolitic appearance. Undulations have amplitudes of 1 cm and wave lengths of 4 to 6 cm. Veinlets or stylolitic zones are at 30° from horizontal. Infilled fractures at 4.55 ft and 4.7 ft are en echelon
4.6	5	Polyhalitic anhydrite, moderate reddish-brown (10R5/2); more fissile. Interlayers are moderate orange-pink (10R7/4). These may be infilled bedding-plane fractures. Many partially infilled horizontal fractures (1 mm wide). Some higher angle fractures. At 4.9 ft a marbled or spotted zone of mixed very pale blue-green (5BG8/2) anhydrite and moderate reddish-brown (10R5/2) polyhalitic anhydrite. Strongly fissile
5	5.3	Anhydrite, very pale blue-green (5BG8/2). Deformed layers in polyhalitic anhydrite, moderate reddish-pink (10R7/6). Deformation of layers consists of pullaparts, necking and thinning. Infilled fractures crosscut layering; fractures are partially open
5.3	5.5	Anhydrite, very pale green (5BG8/2). Deformed layers with marbled appearance with polyhalitic anhydrite, moderate reddish-pink (10R7/6). Subhorizontal lenses of halite (5 × 1 cm). Vertically aligned halite pseudomorphs after gypsum or anhydrite. Infilled fractures, moderate orange-pink (10R7/4)

Hole No. 2, Box No. 3

5.5	6.1	Anhydrite, pale blue-green (5BG8/2), interlaminated with polyhalitic anhydrite, moderate reddish-orange (10R7/6). Blue-green anhydrite layers show pullapart and necking structures. Pullaparts are infilled with reddish polyhalitic anhydrite; horizontal patches of halite
6.1	-	Infilled 1-mm-wide fracture, near horizontal, that crosscuts earlier structures
6.1	6.4	Massive polyhalitic anhydrite, moderate reddish-orange (10R7/6), with faint lamination. Towards contact below with halite there is an incoming of subhorizontal patches of halite, moderate reddish-brown (10R4/4)
6.45	-	Contact, halite, moderate reddish-orange (10R4/4), with anhydrite, light bluish-grey (5B7/1)

<u>Depth (ft)</u>		<u>Core Description</u>
<u>From</u>	<u>To</u>	
6.45	6.9	Anhydrite, light bluish-grey (5B7/1), with halite patches, yellowish-grey (5Y7/2). Distinct sub-horizontal fractures, 1 mm wide, partially infilled. Infilled vertical fractures, <1 mm wide. Near contact, at bottom of segment, clay lies along fracture surfaces. Blue-grey anhydrite is broken up in upper portion. Fractures are infilled with pale greyish-orange (10YR8/3) alteration mineral (?)
6.9	7	Halite, medium olive-grey (5Y5/1); medium grain size. Banded, dipping 10°-15° from horizontal. Intergranular anhydrite
7	7.3	Anhydrite, pale bluish-grey (5B8/1), massive. At 7.15 ft and 7.2 ft, dipping 1- to 5-mm-wide halite-infilled fractures. Fractures bifurcate and interbraid. Some cross-fibre growth
7.3	7.7	Halite; coarse grain size. Variety of colors and range of grain size. Lower contact of anhydrite at 7.3 ft is inclined but parallel to halite veins above. Clay zone, light grey (N7), at contact

Hole No. 3, Box No. 1

0.0	2	Halite; coarse-grained (1+ cm). Good equilibrium mosaic grain boundaries, medium-grey (N5) to light yellowish-grey (5Y9/1). Color largely controlled by intergranular clay, light bluish-grey (5B7/1), ≤3% of the rock. Hematitic or polyhalitic patches along grain boundaries, moderate reddish-orange (10R6/6) and <1% of rock. Horizontal separations. Many fluid inclusions (3 mm in diameter)
-----	---	---

Hole No. 3, Box No. 2

2	2.3	Halite, light greyish-orange to pink (5YR8/2); very coarse-grained. 1-cm-wide fluid inclusions. Intergranular moderate reddish-orange (10R6/6) polyhalite, 1% of rock. Grain size ~2 cm. Downward there is more intergranular clay
2.3	2.7	Halite, very coarse-grained (~2 cm in diameter), medium light-grey (N6). Many large elongate (>1 cm) fluid inclusions at 2.5 ft. Intergranular moderate reddish-orange (10R6/6) polyhalite <1%. Intergranular patches of clay <1% greyish blue-green (5BG5/2). Parallel horizontal separations
2.7	4	Halite, pale greyish-orange (10YR8/4), very coarse-grained. Intergranular polyhalite (1%), moderate reddish-orange to pink (5YR8/2). Isolated patches of clay (<1 cm) and (<1%) greyish blue-green (5BG5/2). Core is broken up in this interval although complete depth was taken

Hole No. 3, Box No. 3

4	4.25	Contact zone: halite, light greyish-orange to pink (5YR8/2). Polyhalitic anhydrite, with spotted moderate reddish-orange (10R6/6), 10-cm-high mound at contact. Contact is clay-rich. This clay is light bluish-grey (5B7/1). Some clay may have been lost during drilling. The lower anhydrite unit is embayed sharply at the contact
4.25	4.75	Polyhalitic anhydrite, spotted moderate reddish-orange (10R6/6). Spots are ~3 to 5 mm in diameter and form clusters that are laminar in appearance. This planar structure is inclined relative to the room floor, but parallels the limbs of the mound on the upper contact. First appearance of 1-mm-wide horizontal fractures

<u>Depth (ft)</u>		<u>Core Description</u>
<u>From</u>	<u>To</u>	
4.75	5.25	Core is broken up and the recovery is not complete. Polyhalitic anhydrite, spotted moderate reddish-orange (10R6/6). Lamination of spot clusters is horizontal. 1-cm-wide halite patches
5.25	5.75	Polyhalitic anhydrite, moderate reddish-orange (10R6/6). Subhorizontal fracture at 5.3 ft. Styloitic texture that becomes increasingly inclined downward. In segment 5.5 to 5.75 ft a relict light-grey (N7) lamination of anhydrite parallels the styloitic texture. 1- to 3-cm-wide patches of clear halite that are partially aligned. 1- to 2-cm patches or clasts of grey anhydrite, at 5.75 ft subhorizontal but crosscutting halite vein (1 cm wide)
5.75	6	Anhydrite, brecciated light-grey (N7) in matrix of moderate reddish-orange polyhalitic anhydrite. Anhydrite clasts are 1- to 5-cm-wide. All are crosscut by partially filled subhorizontal fractures. Some thin <5 mm clear halite laminae

Hole No. 4, Box No. 1

0.0	0.25	Halite, greyish-orange to pink (10R8/6); medium- to coarse-grained. Clay-rich horizontal laminae greenish-grey (5G5/1)
0.25	0.9	Halite; coarser grain size than halite above. Very light grey (10R7/6). Polyhalite <3%
0.9	-	Clay-rich halite. Horizontal ~2- to 3-cm-wide zone. Distinct fluid inclusions ~3 mm in diameter
0.9	1.4	Halite with intergranular polyhalite. Halite is very light grey (N8) to greyish-orange to pink (10R7/6). Polyhalite (~1%)
1.4	2	Halite with trace of polyhalite and Fe-oxide along horizontal partings where the core separates. Polyhalite and clay also occur along these partings. Halite is medium pinkish-orange (10R8/6)

Hole No. 4, Box No. 2

2	3	Halite, light grey (N7); coarse-grained. ~1% polyhalite. Horizontal partings. Rusty staining on surface
3	3.7	Halite, greyish-orange to red (10R8/6). Intergranular polyhalite <3%. From 3.5 to 3.6 ft, grain boundaries are less sutured. Surfaces appear to be etched. Appearance on an embayed surface follows the horizontal partings
3.6	4	Halite, very light grey (N8), coarse grain size

Hole No. 4, Box No. 3

4	4.5	Polyhalitic anhydrite, moderate reddish-orange (10R6/6), with greyish-orange to pink (10R8/2) laminae <0.5 cm wide. Anhydrite, light grey (N7), relict but overgrown by polyhalitic anhydrite. Such light-grey anhydrite forms horizontal bands
4.5	4.75	Polyhalitic anhydrite, moderate reddish-orange (10R6/6); and anhydrite, light grey (N7). Anhydrite bands become thicker in matrix of polyhalitic anhydrite. Clasts of light-grey anhydrite in polyhalitic anhydrite in lowermost portion of this section
4.75	5	Core broken up, with poor recovery
5	5.75	Polyhalitic anhydrite, moderate reddish-orange (10R6/6), with halite patches (1 cm in diameter) and greyish-orange to pink (10R8/4) bands that are inclined at 30° from horizontal. Many subhorizontal fractures partially infilled by polyhalite (?), moderate orange-pink (5YR8/4)

<u>Depth (ft)</u>		<u>Core Description</u>
<u>From</u>	<u>To</u>	
5.75	6	Halite, moderate reddish-brown (10R4/6); coarse grain size. With patches of moderate reddish-orange halite (10R6/6)
Hole No. 4, Box No. 4		
6	7	Anhydrite, light grey (N7), with laminations and interlaminated with 1-cm-wide halite bands, moderate reddish-orange (10R6/6) to moderate yellowish-brown (10YR5/4). Grey laminations in anhydrite unit are broken up or undulatory. At 6.25 ft a very pale orange (10YR8/2) vein occurs. Vein is folded and exhibits extension gaps infilled with halite, boudinage, and folding
7	7.05	Clay zone, very light grey (N8)
7.05	7.25	Halite, moderate orange to pink (5YR8/4), with intergranular polyhalite. At 7.2 ft polyhalite-rich banding appears
7.25	8	Halite, very light grey (N8); very coarse grain size
Hole No. 5, Box No. 1		
0.0	0.9	Halite, very pure, clear to very light grey (N8); coarse grain size. <1% intergranular clay and polyhalite ± hematite
0.9	1.5	Halite, very light grey (N8); coarse grain size, with polyhalite, moderate orange to red (10R7/6), and clay, medium greenish-grey (5G5/1). Polyhalite and clay form discontinuous horizontal bands 0.5 mm wide. Horizontal separations. Clay patches on partings
1.5	2.2	Halite, very light grey (N8) to greyish-red to orange (10R8/6); coarse grain size. Equilibrium grain boundaries. Intergranular polyhalite (3% of the rock), moderate orange to red (10R7/6). Some polyhalite patches are 0.5 cm wide. Clay (<1%), medium greenish-grey (5G5/1)
2.2	2.75	Halite, very light grey (N8) to greyish-red to orange (10R8/6); medium to coarse grain size. Distinct banding. Halite exhibits shape fabric perpendicular to banding. Bands are 1 to 3 cm wide. Discontinuous and subhorizontal. Bands are composed of polyhalite (50%), moderate orange to red (10R7/6). Clay (40%), greenish-black (5G2/1). Anhydrite (?), greyish-orange to pink (10R7/4)
Hole No. 5, Box No. 2		
2.9	4.1	Halite, very light grey (N8) to greyish-red to orange (10R8/6). Intergranular hematite and polyhalite, moderate reddish-orange (10R6/6). Patches are 0.5 cm in width. Clay patches, greenish-grey (5G6/1). Clay and polyhalite are <5% of the rock. Horizontal separations (1 cm apart). Separations still have some strength. If the separations are pulled apart by hand, lenticular clay patches and a white fine-grained mineral, either milled halite or anhydrite, are observed on the separation surface
4.1	4.4	Contact zone between halite (above) and polyhalitic anhydrite (below) of MB139. Contact is an undulatory surface (amplitude up to 3 cm and wavelength of 15 cm). Laminae of clay at contact. Clay is very light bluish-grey (5B7/1). Inclined band, 5 cm wide, of polyhalitic anhydrite (moderate reddish-orange) (10R6/6). Band consists of densely spotted polyhalitic anhydrite. Spots are 0.1 to 0.5 cm in diameter. Intergranular halite. The band drapes over mounds of hopper crystals. Intergranular to the cluster of hopper crystals is a matrix of either gypsum or anhydrite, light grey (N8)

<u>Depth (ft)</u>		<u>Core Description</u>
<u>From</u>	<u>To</u>	
4.4	4.9	Anhydrite, light-grey (N6), overgrown by spotted patches of polyhalitic anhydrite, moderate reddish-orange (10R6/6). Intergranular to the spotted polyhalitic anhydrite; very fine grain size. This phase may be a second-stage anhydrite. Anhydrite and polyhalitic anhydrite form inclined laminae. Inclined laminae may parallel contact. Elongate growth of secondary anhydrite (?) in the plane of the laminations is observed. Also, intergranular growth of halite is present
4.9	5.5	Polyhalitic anhydrite, moderate reddish-orange (10R6/6) overgrows anhydrite, medium light-grey (N6). Overgrowths are spotted. Polyhalitic anhydrite and anhydrite are also interlaminated. Laminae are horizontal and 1 cm wide, swallow-tail growth structures in which halite has replaced the original gypsum. Swallow tails are 0.5 to 3.0 cm long, vertical to subvertical. The structure grows across and includes previous laminae. Some deformation of the swallow-tail structures is shown by pullaparts infilled by fine-grained white anhydrite

Hole No. 5, Box No. 3

5.5	6.2	Anhydrite, medium light-grey (N6), as laminae that are overgrown by polyhalitic anhydrite, moderate reddish-orange (10R6/6). Polyhalitic bands have spotted appearance. Below 6 ft the grey anhydrite becomes more dominant than the polyhalitic anhydrite. At 5.8 ft a grey anhydrite band is broken up, with the resultant interspace infilled with halite. Below this zone halite is pervasive in the groundmass. At 6 to 6.2 ft halite vein structure is evident, up to 0.5 cm wide and vertical
6.2	6.5	Anhydrite, medium light-grey (N6), and polyhalitic anhydrite, moderate orange to pink (10R7/4), have a marbled appearance and subhorizontal fractures that are infilled with greyish-brown (5YR3/2) mineral (?)
6.5	7	Anhydrite, medium light-grey (N6), nodular and marbled appearance. Portions of the anhydrite are brecciated. Massive fine-grained with medium-grain-size halite zones that have intergranular anhydrite. Orange-pink coloration of above is much less
7	7.5	Anhydrite, light grey (N7), interlaminated with medium-grain-size halite. Laminations are inclined. Laminae are 2.5 cm wide. At 7.5 ft contact with massive anhydrite, medium light-grey (N6). Clay zone at the contact
7.5	8	Halite, light grey (N7) and medium- to coarse-grained, portions of the halite have moderate orange to pink (5YR8/4) laminated appearance that is imparted by clay-rich zones. Lamination is horizontal. Pullaparts of the lamination; e.g., 7.8 to 8 ft. Some isolated inclined laminae where inclination is not reflected in the overlying laminae

DISTRIBUTION:

DOE/TIC-4500, R74, UC-70 (316)

US Department of Energy, Headquarters (3)
Office of Nuclear Waste Management
Attn: Program Manager (WIPP)
Director, Division of Waste Isolation (2)
Washington, DC 20545

US Department of Energy, Headquarters
Office of Defense Waste and By-Products
Attn: Director
Washington, DC 20545

US Department of Energy (2)
Albuquerque Operations
Attn: W. R. Cooper, Mgr, WIPP, Project Office
PO Box 3090
Carlsbad, NM 88221

US Department of Energy
c/o Battelle Office of Nuclear Waste Isolation
505 King Ave
Columbus, OH 43201

Battelle Memorial Institute
Office of Nuclear Waste Isolation
Attn: S. Goldsmith, Mgr, ONWI Library
505 King Avenue
Columbus, OH 43201

Battelle Memorial Institute
Project Management Division
505 King Avenue
Columbus, OH 43201

Bechtel National, Inc. (2)
Attn: D. L. Ledbetter
D. Roberts
Fifty Beale St
PO Box 3965
San Francisco, CA 94119

Stanford University
Department of Geology
Attn: K. B. Krauskopf, Chairman
Stanford, CA 94305

Oak Ridge National Laboratory
Attn: J. O. Blomeke
PO Box X
Oak Ridge, TN 37830

US Geological Survey
Water Resources Division
Attn: J. D. Bredehoeft
Western Region Hydrologist
345 Middlefield Rd
Menlo Park, CA 94025

Karl P. Cohen, Consultant
928 N California Ave
Palo Alto, CA 94303

Fred M. Ernsberger, Consultant
1325 NW 10th Ave
Gainesville, FL 32605

Johns Hopkins University
Department of Earth Sciences
Attn: H. P. Eugster
Baltimore, MD 21218

University of New Mexico
Department of Geology
Attn: R. C. Ewing
Albuquerque, NM 87131

University of Minnesota
Department of Civil and Mineral Engineering
Attn: C. Fairhurst
Minneapolis, MN 55455

University of Texas
Department of Geological Sciences
Attn: W. R. Muehlberger
Austin, TX 78712

Vanderbilt University
Department of Environmental Engineering
Attn: F. L. Parker
108 New Engineering Building
Nashville, TN 37235

D'Arcy A. Shock, Consultant
233 Virginia
Ponca City, OK 74601

WIPP Public Reading Room
Attn: G. Schreiner
Atomic Museum, KAFB East
Albuquerque, NM 87185

Carlsbad Municipal Library
WIPP Public Reading Room
Attn: L. Hubbard, Head Librarian
101 S. Hallagueno St
Carlsbad, NM 88220

Thomas Brannigan Library
Attn: D. Dresp, Head Librarian
106 W Hadley St
Las Cruces, NM 88001

Roswell Public Library
Attn: N. Langston
301 N Pennsylvania Ave
Roswell, NM 88201

Hobbs Public Library
Attn: M. Lewis, Librarian
509 N Ship St
Hobbs, NM 88248

State of New Mexico (2)
Environmental Evaluation Group
Attn: R. H. Neill, Director
320 Marcy St
PO Box 968
Santa Fe, NM 87503

NM Department of Energy and Minerals (2)
Attn: L. Kehoe, Secretary
K. LaPlante, Librarian
PO Box 2770
Sante Fe, NM 87501

Emery C. Arnold
New Mexico State Geologist
PO Box 2860
Sante Fe, NM 87501

New Mexico State Library
Attn: I. Vollenhofer
PO Box 1629
Sante Fe, NM 87503

New Mexico Tech
Martin Speer Memorial Library
Campus St
Socorro, NM 87801

University of New Mexico
Zimmerman Library
Attn: Z. Vivian
Albuquerque, NM 87131

USGS, Water Resources Division (2)
505 Marquette, NW
Western Bank Bldg, #720
Albuquerque, NM 87102

USGS, Conservation Division
Attn: W. Melton
PO Box 1857
Roswell, NM 88201

USGS, Special Projects Branch (2)
Attn: R. P. Snyder
Federal Center, Bldg 25
Denver, CO 80225

NM Bureau of Mines and Mineral Resources (2)
Attn: F. E. Kottowski, Director
Socorro, NM 87801

Klaus Kuhn
Gesellschaft fuer Strahlen-und
Umweltforschung MBH Muenchen
Institut fuer Tieflagerung
Berliner Strausse 2
3392 Clausthal-Zellerfeld
FEDERAL REPUBLIC OF GERMANY

Klause Eckart Maass
Hahn-Meitner-Institut fuer Kernforschung
Glienicke Strasse 100
1000 Berlin 39
FEDERAL REPUBLIC OF GERMANY

Michael Langer
Bundesanstalt fuer Geowissenschaften und Rohstoffe
Postfach 510 153
3000 Hanover 51
FEDERAL REPUBLIC OF GERMANY

Helmut Rothemeyer
Physikalisch-Technische Bundesanstalt
Bundesalle 100
3300 Braunschweig
FEDERAL REPUBLIC OF GERMANY

Rolf-Peter Randl
Bundesministerium fuer Forschung und Technologie
Postfach 200 706
5300 Bonn 2
FEDERAL REPUBLIC OF GERMANY

Fenix & Scisson, Inc.
Attn: J. A. Cross
3170 W Sahara Avenue
Spanish Oaks D-12
Las Vegas, NV 89102

Gayle Pawloski, L-222
Geologist CSDP
Lawrence Livermore Laboratory
Livermore, CA 94550

US Nuclear Regulatory Commission (3)
Division of Waste Management
Mail Stop 69755
Attn: J. Martin
M. Bell
H. Miller
Washington, DC 20555

Center of Waste Management Programs
Department of Social Sciences
Attn: G. L. Downey
Michigan Technology University
Houghton, MI 49931

Department of Geological Sciences
Attn: D. W. Powers
University of Texas at El Paso
El Paso, TX 79968

UCLA
Department of Earth and Space Sciences
Attn: J. Rosenfeld
Los Angeles, CA 90024

University of Texas
Department of Geological Sciences
Attn: J. K. Warren, Ph.D.
Assistant Professor
PO Box 7909
Austin, TX 78712

6000 E. H. Beckner
6253 J. C. Lorenz
6330 W. D. Weart
6331 D. J. Borns (11)
6331 S. J. Lambert
6331 A. R. Lappin
6331 K. L. Robinson
6331 S. E. Shaffer
6331 C. L. Stein
6332 Sandia WIPP Central Files (12)
7111 L. J. Barrows
7133 R. D. Statler
7135 P. D. Seward
8024 M. A. Pound
3141 C. M. Ostrander (5)
3151 W. L. Garner (3)